IMAV2017-42
http://www.imavs.org/pdf/imav.2017.42

Investigation on Boundary Layer Ingestion Propulsion for UAVs

L. Teperin,* M. El-Salamony,† A. Moharam,‡ and M. Shehata§
* Central Aerohydrodynamic Institute (TsAGI),
Zhukovsky street, 1, Zhukovsky, 140180, Russia.
Moscow Institute of Physics and Technology,
Department of Aeromechanics and Flight Engineering,
Gagarina street, 16, Zhukovsky, 140180, Russia.

ABSTRACT

Power reduction is one of the most current important issues. One promising way is to use boundary layer ingestion propulsion. In order to evaluate the benefits of using boundary layer ingestion propulsion in reduction of power consumption and to understand the difference between the propeller placed behind and in front of a fuselage, a comparison is made between propeller placed behind and in front of a fuselage. It is found that the backward position has less drag and power consumption. Power saving coefficient reached 21.7% compared to the forward position and drag coefficient is 28.5% less. Also it shows tendency to stabilize and prevent separation of the boundary layer.

1 INTRODUCTION

Current trends in unmanned aerial vehicles (UAV) market heads to power reduction. One promising method is boundary layer ingestion (BLI) propulsion. The fundamental principle of BLI propulsion is that a propulsor ingests and reaccelerates airframe boundary layer which reduces the wake deformation downstream and jet kinetic energy for the same net force which decreases the power to be added to the flow by propulsor.
The interaction between a propeller and a body has both benefits and drawbacks. The advantages on power consumption can be explained using Froude model of propeller. For the same thrust, the propeller consumes less power if the incoming flow velocity is less. By placing the propeller in a boundary layer or a wake of a body, the incoming flow will have less velocity compared to the free stream, so the power consumption decreases and propulsive efficiency increases. Efficiency can even exceed 100% since the reference velocity is the free stream velocity which is higher than the actual incoming velocity to the propeller. Another useful point is that the power is a function of the difference between inlet and outlet velocities squared, this counted as a benefit for the power reduction since the incoming flow is not uniform, so the exit velocity can be shaped to give the minimum power consumption.
On the other hand, imposing a propeller in the vicinity of a lifting body will affect the boundary layer and the pressure distribution. Air suction near the trailing edge will create low pressure zone and so the pressure drag on the body will increase and the flow will accelerate. Flow acceleration will increase the shear force and so the friction drag will increase. Also the angle of attack must increase to compensate the losses of lift, which also will increases drag. Losses in lift occurs due to the acceleration if the flow under the body, which will decrease the pressure difference in the vertical direction and consequently lift decreases. These effects hold for axisymmetric bodies except the fact that it generates no lift.
Regarding the effects on the boundary layer and the laminar-turbulent transition, this region will be shifted downstream due to presence of negative pressure gradient zone near the trailing edge, and hence, drag will decrease, but this effect is negligible compared the increment of friction drag due to flow acceleration. By using some numerical investigations using panel method combined with integral boundary layer equations, it was found that BLI propulsor under some considerations can prevent boundary layer separation.
This article considers the integration between fuselage and BLI propeller and their mutual effects on the power consumption, drag, and boundary layer properties for the case of cruise flight. It answers two main questions: is it advantageous to integrate them from the power consumption point of view and what is the impact of the propeller position on the flow field.
To understand the effect of the BLI propeller on the power saving, two propeller positions are studied: behind and in front of the fuselage. To study the aerodynamic effect of the BLI propeller on the body, a comparison is conducted between body with and without BLI propeller.

2 LITERATURE REVIEW

Integration between propulsor and a body was studied theoretically in many papers. Smith [1] proved analytically that for the case of a flat plate, propulsive efficiency working

*Email address: teperin@mail.ru
†Email address: elsalamony.mostafa@phystech.edu
‡Email address: a.moharam@phystech.edu
§Email address: moamen.shehata@phystech.edu

on the wake of a flat plate is 127% and power saving about 20%. Teperin and Ujuhu of TsAGI [2] investigated the effect of interference with propeller glider aircraft without considering viscosity. Later, a similar problem has been solved numerically for a propeller mounted at the stern of an airship [3]. In [4] the useful interference between free stream propeller and wing is considered in more detail. Recently, Teperin et al. [5] considered the optimal pressure difference distribution across the propeller to decrease power consumption, and the results shown that the power saving reached more than 20% in comparison of propeller with uniform pressure difference. Drela of MIT [6] derived an analysis of compressible viscous flow around a body with engine based on the mechanical power and kinetic energy instead of the regular forces and momentum flow method, and he explained how to quantify the boundary layer and wake ingestion benefits.
Many experiments were carried out on several bodies as airships where Stern-mounted propellers were investigated as a way to improve the propeller efficiency significantly and reduce its power consumption, but they are directed towards airships and large aircraft. In the experiment of McLemore of NASA [7] they achieved propulsive efficiency of 103%. Goldschmit of NASA [8] found that 50% of power could be saved using BLI and counter rotating propellers as in the experimental aircraft Douglas XB-42 Mixmaster.
Concerning the current development for the future aircraft, the conceptual project of Double Bubble (D8) of MIT, NASA, and Boeing [9] has fuel saving of 33% compared to the optimized conventional configuration having the same technology level using BLI and another techniques. ONERA [10] also achieved 23% of power saving in wind tunnel experiments for a similar project with Airbus.
Interaction between BLI propulsor and airfoil is considered in [11]. Main findings are that BLI affects mainly the pressure-dependent parameters. It is found that drag increased for the given flight conditions 11.4% divided as increment in friction drag 2.11% and 16.07% in pressure drag and lift decreased 8.89%. On the other hand, the power is reduced by 14.4% as compared to the free-stream propulsor, and the propulsive efficiency reached 109% and it was concluded that BLI is useful from the viewpoint of power saving
Similar work is done in [12] in more detail. it was found that boundary layer became more laminar and the boundary layer thickness decreased, the momentum and energy losses decreased, the flow in the leading part of the airfoil is not changed, and the friction drag can be neglected with respect to pressure drag.
The optimal distribution of the pressure difference across the active disk of propeller for minimum power consumption is developed in[5]. It was depicted that propeller with optimum pressure difference placed in the rear part of airship shows reduction in consumed power more than 20% when compared to propeller with uniform pressure difference.
Numerical investigations made by Lutz T. et al. [7] using panel method combined with integral boundary layer equations found that BLI propulsor under some considerations can prevent boundary layer separation.
Considering experiments for small bodies, an experiment was conducted by Sabo and Drela in MIT [13] as a proof of concept for the boundary layer ingestion concept. Electric ducted fan propulsor behind a NACA 0040 body of revolution is examined at a Reynolds number of approximately 2.4e5. Wind tunnel air velocity was 13.4 m/s and length of the body was 0.25 m. Measurements showed power savings reached 26% for untripped flow case and 29% for tripped flow case. Also it is found that power saving increases when the propeller is placed closer to the body and when the propulsor is aligned in the same axis of symmetry for the body.
Another experimental study conducted in Lv et. al in TU Delft [14] using the Stereoscopic Particle Image Velocimetry for the first time to visualize the flow field at the location of interaction between a propeller and an incoming body wake and to quantify the terms of power balance method. Results show that one of the main mechanisms responsible for the claimed efficiency enhancement in the experimental setup is due to the utilization of body-wake energy by the wake-ingesting propeller. Shaft power was reduced in the case of wake ingestion by 10% and by 18% for Boundary layer ingestion.

3 THEORETICAL APPROACH

3.1 *Free stream propeller*

Froude model can be used for modelling the free stream 2-D propeller – shown in Figure 1– where the propeller is a zero-thickness disk that creates pressure difference converted at the far field to velocity difference producing thrust. The flow is assumed to be axisymmetric, inviscid, without mixing at the jet edges. Thrust is calculated by the following integration[1]:

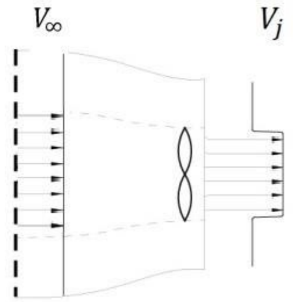

Figure 1: Constant inlet conditions for propeller

$$T = \iint \rho * V_j * (V_j - V_\infty) dA \tag{1}$$

For constant parameters this integration leads to

[1] It is notable that all of the integrations in this section are made on Trefftz plane where pressure is equal to the undisturbed upstream pressure.

IMAV2017-42
http://www.imavs.org/pdf/imav.2017.42

$$T = \dot{m} * (V_j - V_\infty) \tag{2}$$

Propulsive power added is the difference between the kinetic energies of the stream tube passes by the propeller downstream and upstream the propeller, it is calculated as

$$P_p = \iint \frac{1}{2} * \rho * V_j * (V_j^2 - V_\infty^2) dA \tag{3}$$

And for constant parameters this integration leads to

$$P_p = \frac{\dot{m}}{2} * (V_j^2 - V_\infty^2) \tag{4}$$

The propulsive total power (Equation 3) can be decomposed by the Power Balance Method [6] into two categories; thrust (useful) power which is represented by multiplication of thrust by the incoming velocity Equation (5) and wake power due to the velocity perturbations downstream. This wake requires excess energy to be flattened by the flow viscosity. This power is directly proportional to the velocity difference as shown in Equation 6.

$$T * V_\infty = \iint \rho * V_j * V_\infty * (V_j - V_\infty) dA \tag{5}$$

$$E_{wake,prop} = \iint \frac{1}{2} * \rho * V_j * (V_j - V_\infty)^2 dA \tag{6}$$

Propulsive efficiency is defined as the useful power thrust multiply velocity divided by propulsive power (total power). By some mathematics we get the well-known Froude formula

$$\eta = \frac{2 * V_\infty}{V_j + V_\infty} \tag{7}$$

And considering the power decomposition we get

$$\eta = \frac{T * V_\infty}{T * V_\infty + E_{wake,prop}} \tag{8}$$

It is notable that the actual power is more than the calculated power because of the viscous and induced losses.

3.2 Drag Characteristics

Drag is the momentum losses between upstream and downstream flows of a stream tube passes around a body according to the momentum equation [15] as shown in Figure 2. Therefore, it can be calculated directly from the velocity distribution of the wake by the following formula

$$D = \iint \rho * V_w * (V_w - V_\infty) dA \tag{9}$$

This force can be represented in form of power consumed as drag multiplied by the upstream velocity

$$D * V_\infty = \iint \rho * V_w * V_\infty * (V_w - V_\infty) dA \tag{10}$$

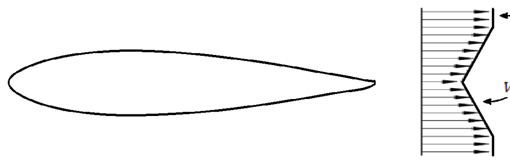

Figure 2: Airfoil and velocity distribution of the wake.

This power is consumed due to two reasons: dissipation in the viscous boundary layer and velocity perturbation in the wake. The dissipated energy in the boundary layer is quantified as the energy losses between upstream and downstream in the stream tube that passes around the airfoil, which is equal to:

$$\phi_{BL} = \iint \frac{1}{2} * \rho * V_w * (V_\infty^2 - V_w^2)) dA \tag{11}$$

While the energy of the wake can be quantified by the perturbations in the stream tube and calculated by the following equation:

$$E_{wake,body} = \iint \frac{1}{2} * \rho * V_w * (V_\infty - V_w)^2 dA \tag{12}$$

And hence, the total consumption in kinetic energy is the summation of the BL dissipation and the wake perturbations which are equal to the drag power

$$D * V_\infty = E_{wake,prop} + \phi_{BL} \tag{13}$$

3.3 Ideal BLI Propulsor

The concept of the ideal Boundary Layer Ingestion Propulsor is to make use of the BL air and reenergize it to generate the same amount of thrust but by less power. In addition, the BLI propulsor will 'fill' the momentum gap generated by the body due to drag and so it will minimize the wakes created by the body and the propeller downstream which will decrease the losses in kinetic energy very much as shown in Figure 3. Moreover, the free stream propulsor obtain thrust by accelerating the free stream which will generate propulsor wake downstream which absorbs energy also.

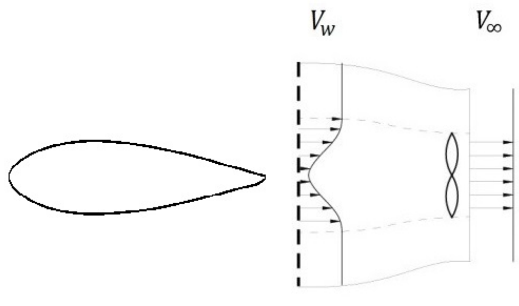

Figure 3: Perfect boundary layer Ingestion.

In the ideal case, all the wake will be ingested and flattened, the jet velocity will exactly match the undisturbed velocity. Thus, the only energy dissipated will be due to the BL viscosity which is defined by Equation 11. Since the stream tube is accelerated to the upstream conditions and all the wake is eliminated, the kinetic energy added by the propulsor to the stream tube will be equal only to the losses in the boundary layer, which can be evaluated as the difference in kinetic energy of the flow in front of and behind the body as in the following equation:

$$E_{prop,BLI} = \iint \frac{1}{2} * \rho * V_w * (V_\infty^2 - V_w^2) dA \tag{14}$$

So the required power decreased while the drag and thrust still exist with the same value.
One main important parameter used to quantify the benefits of BLI is the power saving coefficient which is defined as in the following equation

$$PSC = \frac{P_{noBLI} - P_{BLI}}{P_{BLI}} \tag{15}$$

Concerning the efficiency of this system, the propulsive efficiency is still defined as the useful power (thrust multiply velocity) divided by total power. Since thrust is equal to drag, we can replace the numerator to be $D * V_\infty$. By using Equation 13 the efficiency in will be

$$\eta = \frac{D * V_\infty}{E_{prop,BLI}} = \frac{\phi_{BL} + E_{wake,prop}}{\phi_{BL}} > 1 \tag{16}$$

4 Problem Description

Investigation is conducted using Computational Fluid Dynamics package Ansys CFX 17.2 using RANS equations and a Shear Stress Transport (SST) turbulence model.

4.1 Geometry

The fuselage is modelled as axisymmetric body of NACA 0024 cross section with length of 0.5 m and the propeller is modelled using active disk theory with radius is 0.05 m, which corresponds to 10% of length, placed with two configurations: 0.02 m behind the trailing edge of the fuselage, and 0.02 m in front of the fuselage which corresponds to 4% of chord.

4.2 Mesh Description

A cylindrical domain was considered of width 6 m and height of 2 m revolved by 1^o. The fuselage is placed 2 m apart from the domain inlet. A body of influence is made with dimensions of 1.9 m width and 0.52 m height and the distance between the fuselage nose and the rectangle is 0.52 m as shown in Figures 4 and 5.

The airfoil has number of divisions equals to 200 and the propeller has 40 for each edge. Element size in the body of influence is 0.005 and the growth rate is 1.04. The mesh has total number of nodes and elements 149401 and 521680 respectively. Shown in Figures 6 and 7 the mesh around the body and the active section in forward and backward configurations respectively.

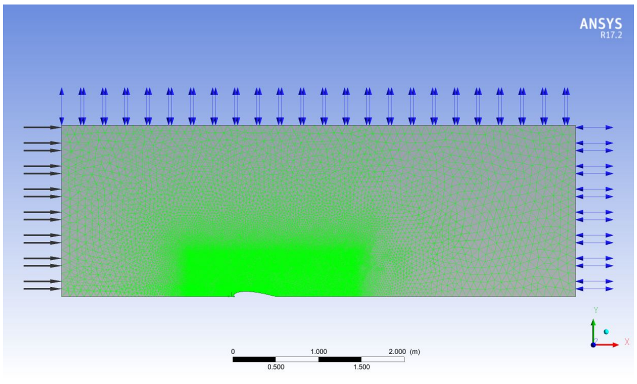

Figure 4: Computational domain for the studied case.

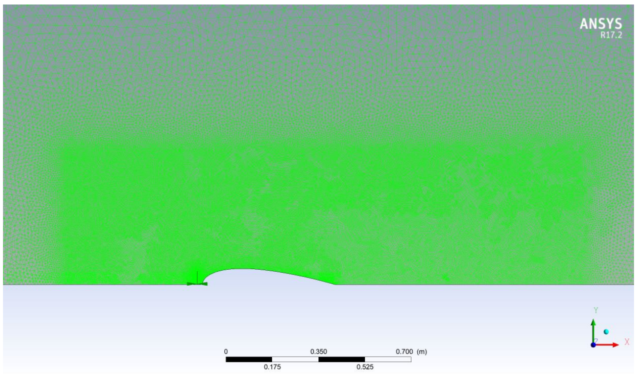

Figure 5: Body of influence around the studied body.

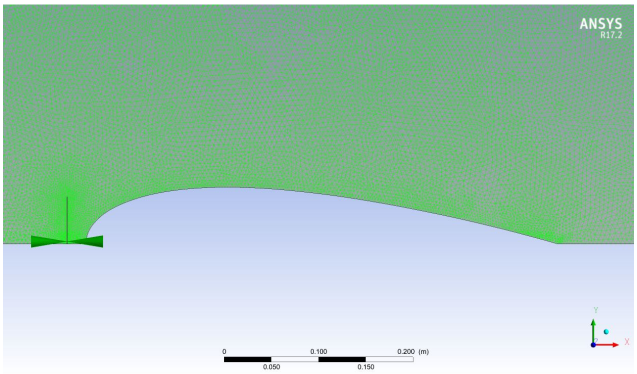

Figure 6: Computational mesh around the body and the active section in forward configuration.

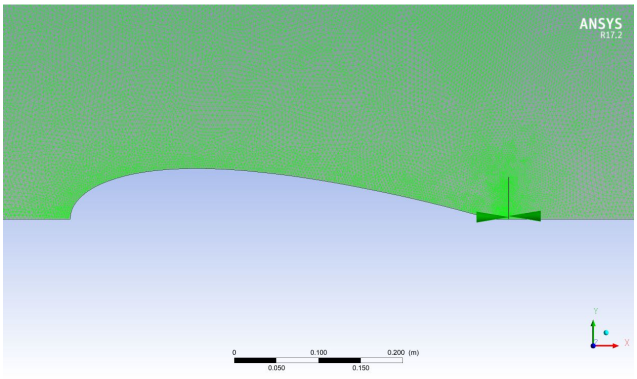

Figure 7: Computational mesh around the body and the active section in backward configuration.

4.3 Boundary Conditions

CFD calculations are sensitive to the boundary conditions. These conditions affect the stability and convergence of the solution and have impact on the physics of the simulated case. The BCs must generate flow compatible with the physics of the flow and the theory used for modelling.
The boundary condition of the body is no-slip wall. Propeller is set to have pressure difference boundary condition to provide thrust equals to drag. Pressure difference across the propeller is calculated by Equation 17.

$$\Delta P_i = \Delta P_{i-1} + \frac{D-T}{S_{prop}} \times K \tag{17}$$

where ΔP_i and ΔP_{i-1} are the pressure difference across the propeller in the current and previous iterations, S_{prop} is the propeller area and K is a relaxation factor. All boundary conditions are listed in the table below.

Boundary	Condition
Inlet	Velocity Inlet
Side Wall	Symmetry
Fuselage	No-Slip wall
Propeller	Pressure difference
Exit	Opening

Table 1: Boundary conditions

Pressure and temperature are set to be 1 bar and 15^{o}C respectively. Free stream velocity is 10 m/s (to be far from the compressibility effect). Angle of attack is kept zero since only the axisymmetric case is considered.

5 Results and Discussion

For the forward propeller position, thrust is set to be equal to the profile drag. Equation 3 can be used to find the required power. The results show that required power is 1.008 W, mass flow rate= 0.0828 kg/s, pressure ratio = 1.25 and the drag coefficient is 0.0147 divided to 57.12% of pressure drag and 42.88% of friction drag.
Same procedure is also done for the backward propeller position. The results show that required power is 0.792 W, mass flow rate= 0.091 kg/s, pressure ratio = 1.18 and the drag coefficient is 0.0104 divided to 50.5% of pressure drag and 49.5% of friction drag.
By comparing the two configurations, it is found that the propeller located after the fuselage will cause less drag (28.5% less). The consumed power is also decreased and the power saving coefficient reached 21.74%.Moreover, BLI ingests more mass flow rate and apply less pressure ratio which is beneficial for the durability of the propeller.

Position	C_D	Energy $[W]$
Backward	0.0104	0.799
Forward	0.0145	1.021

Table 2: Results for backward and forward positions.

For better understanding of the drag increment reason, it is important to investigate how the flow will go past the body. For the forward position, the flow acceleration in the front part of the body is high and reached its maximum value in the maximum thickness position, then the stream tube diverge as its area increases downstream. Due to this a positive pressure gradient is established which eventually leads to flow separation after the maximum thickness position and flow unsteadiness as shown in Figure 8 which leads to massive increment in drag.

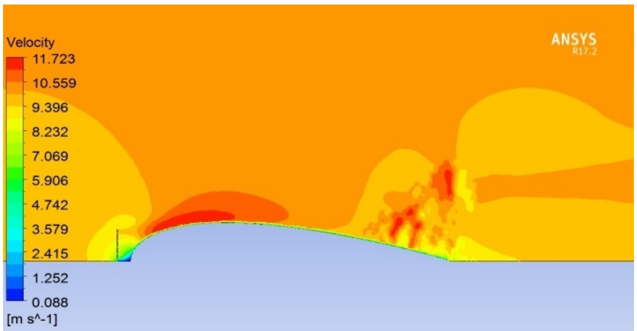

Figure 8: Velocity contour around the body with forward propeller showing unsteady flow.

On the other hand, the backward propeller position, the flow is not forced to accelerate in the front part of the body, it will accelerate in the rear part due to presence of negative pressure gradient created by the propeller. This leads to flow attachment in the rear part of the body as shown in Figure 9.

IMAV2017-42
http://www.imavs.org/pdf/imav.2017.42

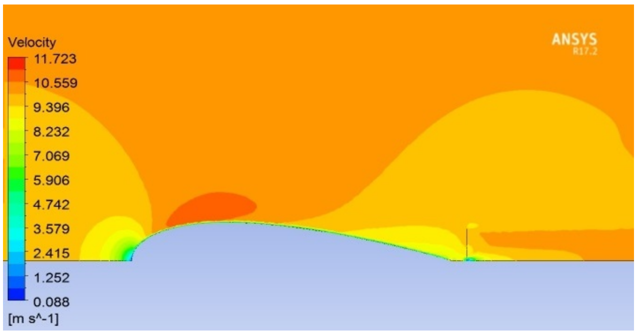

Figure 9: Velocity contour around the body with backward propeller.

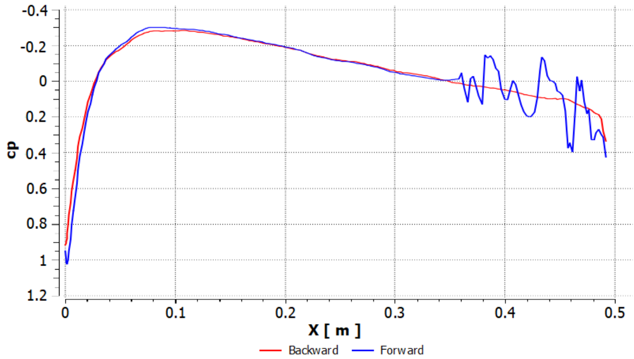

Figure 10: Pressure coefficient distribution on the body wall.

Energy consumption is highly dependent on drag and incoming velocity. For the backward configuration, the required power is less compared to the forward configuration. This is due to two reasons: the backward configuration requires less thrust due to absence of flow separation and the incoming velocity is less as it is affected by the boundary layer of the upstream body. In other words, the stream tube ejected from the propeller does not affect the upstream body in contrast to the forward configuration which will stimulate the flow separation after the maximum thickness position of the body.
Of interest the pressure distribution on the body surface is investigated. As shown in Figure 10 for the case of the forward configuration, the leading edge for the forward configuration faces higher pressure than the backward pressure because of the propeller jet is concentrated in this zone as shown in Figure 11. Near the maximum thickness position the forward configuration has higher speed and hence less pressure is applied. Further downstream there is massive pressure disturbance in the rear part of the body as in illustrated in Figures 12 and 13 where velocity contours around the trailing edge of the body are shown for both configurations. Contrarily the backward configuration stabilizes the flow and accelerates the boundary layer and decreases its thickness as shown in Figure 14.

Distribution of velocity components in the trailing edge show big scattering for the forward configuration while the backward one shows smooth behaviour as shown in Figures 15 and 16.

Of interest to study the Power balance Method terms for the backward configuration. Considering the drag terms, BL dissipation ϕ_{BL} was measured according to Equation 11 and it is equal to 3.9226 W. Wake energy $E_{wake,body}$ is evaluated according to Equation 12 and it is found that it equals to 0.102 W. Drag power according to Equation 10 is 4.0246 W which is equal to adding ϕ_{BL} and $E_{wake,body}$ as state in Equation 13. Power consumed by the BLI propeller $E_{prop,BLI}$ is

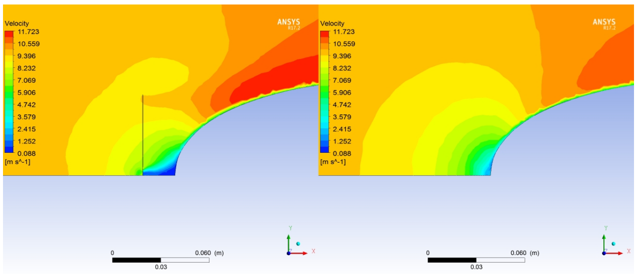

Figure 11: Velocity contour around the nose with forward and backward propeller.

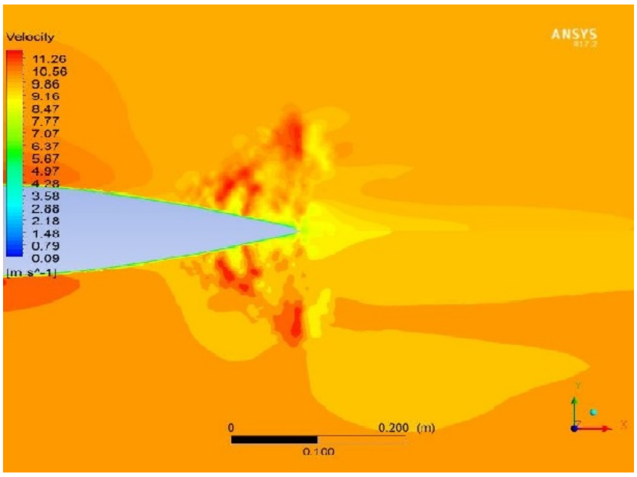

Figure 12: Velocity contour around the tail with forward propeller.

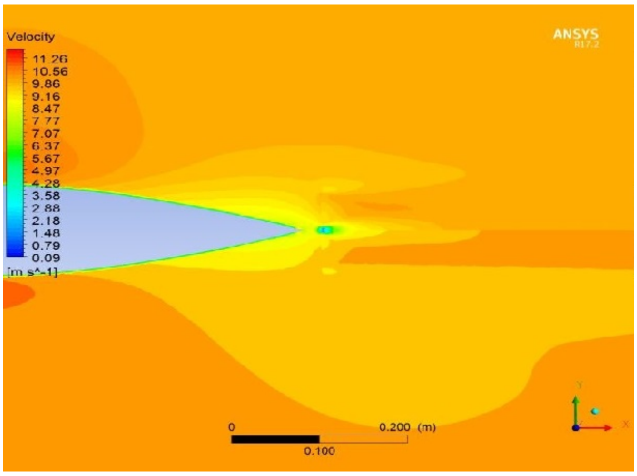

Figure 13: Velocity contour around the tail with backward propeller.

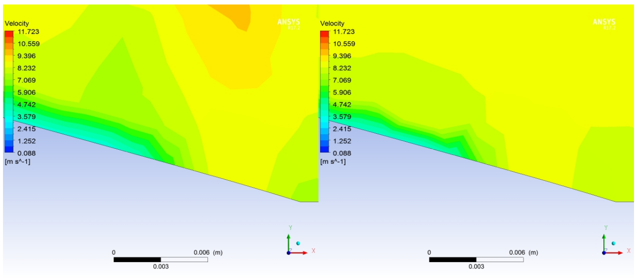

Figure 14: Velocity contour around the tail with forward and backward propeller showing the smaller boundary layer for the backward configuration.

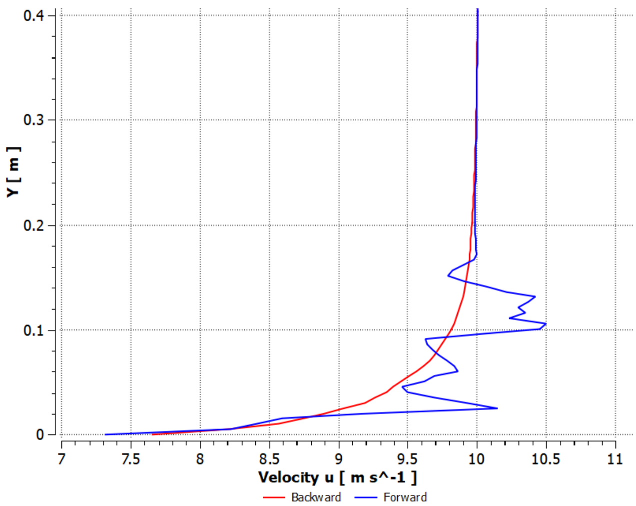

Figure 15: Horizontal velocity component distribution behind the trailing edge.

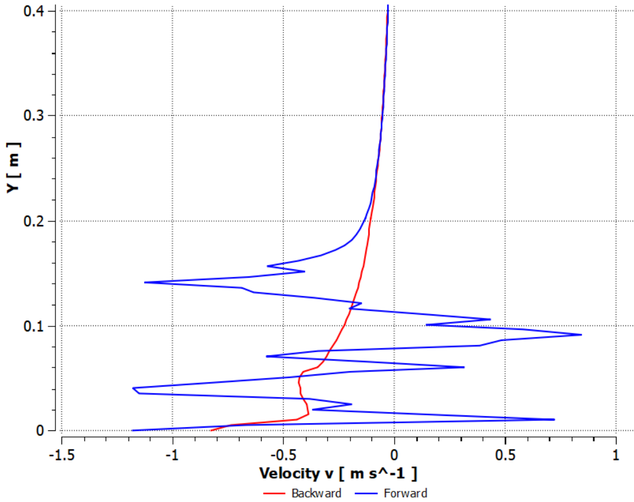

Figure 16: Horizontal velocity component distribution behind the trailing edge.

calculated as in Equation 14, and it equals 3.9804 W. the error between $E_{prop,BLI}$ and ϕ_{BL} is due to a problem in mapping the velocities to Trefftz plan because there is a small zone near the center line of the propeller has negative pressure, which led to imaginary values. it is notable to mention that the integration is made in a line not in a circle. Efficiency (using Equation 16) is calculated and it is 102.6%.

6 Conclusion

Benefits of the boundary layer ingestion and its impact on the aerodynamics of an axisymmetric body are investigated. A comparison is made between propeller placed behind and in front of a fuselage. It is found that the backward position has less drag and power consumption. Power saving coefficient reached 21.7% compared to the forward position. The forward propeller has higher drag because it increases the disturbance in the flow after the maximum thickness position while the backward propeller reduces the turbulence because of the induced negative pressure field. Also BLI propeller ingests more mass flow rate and apply less pressure ratio which is beneficial for the durability of the propeller.
BLI propulsion is favorable because it stabilizes the flow over the body and decrease power consumption.

References

[1] Leroy H Smith. Wake ingestion propulsion benefit. *Journal of Propulsion and Power*, 9(1):74–82, 1993.

[2] L. Teperin and A. Ujuhu. Method for determining pressure drag in aerodynamic interference problems. *TsAGI Science Journal. [in Russian]*, XXI(3):3–10, 1990.

[3] A.A. Razov. Numerical analysis of the efficiency of the location of the propeller in a viscous wake using Navier-

Stokes equations. *TsAGI Science Journal. [in Russian]*, XL(3):60, 2009.

[4] A.V. Kornushenko, O.V. Kudryavtsev, L.L. Teperin, L.N. Teperina, A.V. Shustov, F. Orfinejad, and M. Thein. useing the principle of useful interference to improve the aerodynamic perfection of the layout of the propeller and wing. *TsAGI Science Journal. [in Russian]*, XLVII(8), 2016.

[5] L.L. Teperin, L.N. Teperina, F.E. Orfinejad, M. El-Salamony, and M. Thein. Froude model of ideal propeller in inhomogeneous flow. *TsAGI Science Journal. [in Russian]*, XLVIII(3), 2017.

[6] Mark Drela. Power balance in aerodynamic flows. *AIAA journal*, 47(7):1761–1771, 2009.

[7] H Clyde McLemore. Wind-tunnel tests of a 1/20-scale airship model with stern propellers. Technical report, DTIC Document, 1962.

[8] F. Goldschmied. Aerodynamic design of low speed aircraft with a NASA fuselage/wake propeller configuration. AIAA-86-2693. In *AIAA/AHS/ASEE Aircraft Systems, Design and Technology Meeting*, pages 20–22, 1986.

[9] M Drela. Development of the D8 transport configuration, AIAA 2011_3970, AIAA appl. In *Aero. Conf*, 2011.

[10] Gérald Carrier, Olivier Atinault, Richard Grenon, and Christophe Verbecke. Numerical and experimental aerodynamic investigations of boundary layer ingestion for improving propulsion efficiency of future air transport. In *31st AIAA Applied Aerodynamics Conference*, page 2406, 2013.

[11] S.G. Ignatiev, L.N. Teperina, and M. El-Salamony. On the performance of propeller behind an airfoil at transonic speeds. *TsAGI Science Journal. [in Russian]*, XLVIII(3), pages 3–10, 2017.

[12] M. El-salamony and L. Teperin. 2D numerical investigation of boundary layer ingestion propulsor on airfoil. In *7th European Conference for Aeronautics and Space Sciences*, 2017.

[13] K. Sabo and M. Drela. Benefits of boundary layer ingestion propulsion. In *53rd AIAA Aerospace Sciences Meeting*, page 1667, 2015.

[14] P Lv, D Ragni, T Hartuc, L Veldhuis, and AG Rao. Experimental investigation of the flow mechanisms associated with a wake-ingesting propulsor. *AIAA Journal*, pages 1–11, 2016.

[15] J. Anderson. *Fundamentals of aerodynamics*. Tata McGraw-Hill Education, 2010.